

# Dalton Transactions

Accepted Manuscript



This is an *Accepted Manuscript*, which has been through the Royal Society of Chemistry peer review process and has been accepted for publication.

*Accepted Manuscripts* are published online shortly after acceptance, before technical editing, formatting and proof reading. Using this free service, authors can make their results available to the community, in citable form, before we publish the edited article. We will replace this *Accepted Manuscript* with the edited and formatted *Advance Article* as soon as it is available.

You can find more information about *Accepted Manuscripts* in the [Information for Authors](#).

Please note that technical editing may introduce minor changes to the text and/or graphics, which may alter content. The journal's standard [Terms & Conditions](#) and the [Ethical guidelines](#) still apply. In no event shall the Royal Society of Chemistry be held responsible for any errors or omissions in this *Accepted Manuscript* or any consequences arising from the use of any information it contains.

## ARTICLE

## Switchable Platinum-based Tweezers with Pt-Pt Bonding and Selective Luminescence Quenching

Cite this: DOI: 10.1039/x0xx00000x

Benjamin Doistau,<sup>a,b</sup> Caroline Rossi-Gendron,<sup>a,b</sup> Arnaud Tron,<sup>c</sup> Nathan D. McClenaghan,<sup>c</sup> Lise-Marie Chamoreau,<sup>a,b</sup> Bernold Hasenknopf<sup>\*a,b</sup> and Guillaume Vives<sup>\*a,b</sup>

Received 00th January 2012,  
Accepted 00th January 2012

DOI: 10.1039/x0xx00000x

www.rsc.org/

Molecular tweezers incorporating peripheral platinum salphen complexes and a central chelating terpyridine group have been synthesized. The terpyridine can be switched upon metal binding between a free 'W' shaped form and a coordinated 'U' form. The crystallographic structure of the zinc-closed molecular tweezers was obtained and presented a strong  $\pi$ -stacking between the Pt-salphen units associated with a Pt-Pt bond. The luminescence properties, notably in response to selected guest ions ( $\text{Zn}^{2+}$ ,  $\text{Pb}^{2+}$ ,  $\text{Hg}^{2+}$ ) and the resulting mechanical motion, have been investigated by UV-Vis and emission spectroscopy. While ion coordination to the terpy resulted in no significant changes in the luminescence, a selective intercalation of a second  $\text{Hg}^{2+}$  associated with a large differential quenching was observed.

### Introduction

In the field of nanosciences, the search for new molecules displaying switchable properties<sup>1</sup> attracts the interest of synthetic chemists and nanotechnologists as it provides new objects that operate at the sub-nanometre level.<sup>2</sup> This endeavour has led to the development of a variety of molecular machines inspired by their macroscopic counterparts such as molecular motors,<sup>3</sup> switches,<sup>4</sup> shuttles,<sup>5</sup> turnstiles,<sup>6</sup> nanovehicles<sup>7</sup> and tweezers.<sup>8</sup> Different stimuli, such as pressure, temperature or light have been used to switch optical or magnetic properties, however the use of a mechanical motion to effect change is an innovative approach. Supramolecular chemistry appears to be a key element to build switchable systems. Among the family of molecular machines, molecular tweezers<sup>8a, 8b</sup> are good candidates to perform such tasks.

The term 'molecular tweezers' was first introduced by Whitlock<sup>9</sup> to define a molecular receptor characterized by two flat, generally aromatic, identical pincers separated by some more or less rigid spacers. Depending on the flexibility of the spacer different recognition properties can be obtained. Rigid or semi-flexible spacers have so far been the most used in molecular tweezers design, mainly for molecular recognition purposes. However stimuli-responsive spacers using redox,<sup>10</sup> photochemical<sup>11</sup> or ion coordination<sup>12</sup> triggers have been recently used to control switchable molecular tweezers and construct molecular machines or devices.

We are particularly interested in the design of molecular tweezers switchable by metal coordination.<sup>13</sup> Our system, inspired by the work of Lehn<sup>12a-f</sup> is based on a terpyridine

(terpy) ligand substituted in 6 and 6' positions by two arms bearing molecular recognition moieties (Fig 1). The terpyridine can switch upon metal coordination between a "W" shaped open form and a "U" shaped closed form, bringing the two recognition units in close proximity enabling substrate binding. Upon decoordination the tweezers will reopen, releasing the intercalated substrate. The recognition units are based on Pt-salphen complexes with luminescent properties that could act as probes for the intercalation of substrates<sup>14</sup> or ions.<sup>15</sup> We have recently synthesized Pt-salphen tweezers<sup>16</sup> with tert-butyl groups on the salen unit to increase solubility (Fig 1), however no intercalation of flat aromatic substrates was observed probably due to the steric hindrance of the tert-butyl groups preventing  $\pi$ -stacking interactions. In this work, we decided to reduce their number and move them away from the salphen complex via alkyne spacers (Tweezers **1** in Fig 1). In this case, a higher capacity to interact with aromatic substrates or platinum complexes via the formation of Pt-Pt bonds was anticipated.

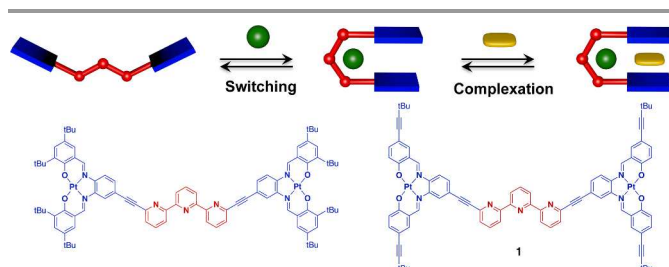


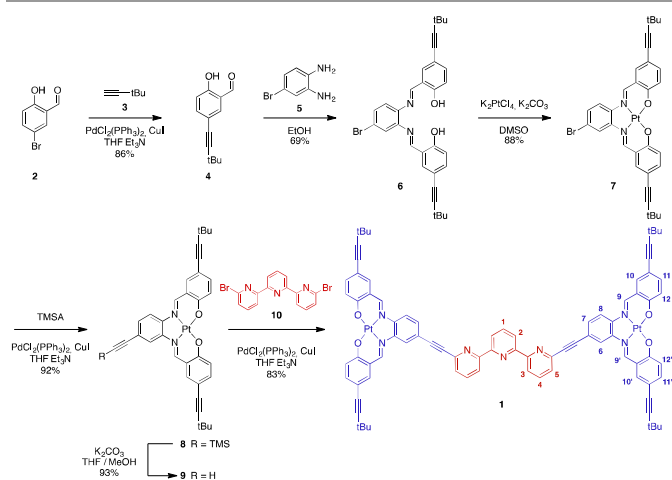
Fig 1. Schematic principle of the molecular tweezers (top) and molecular representation of synthesized tweezers (bottom).

The synthesis of the Pt-based molecular tweezers is presented here, as well as their reversible switching and molecular recognition properties. Luminescence studies of the open and closed tweezers in solution and in the solid state are also presented.

## Results and discussion

### Synthesis

The molecular tweezers **1** were synthesized in a modular fashion using a "chemistry on complex" strategy with Pd cross-coupling reactions (Scheme 1). First, the extended tert-butyl groups were introduced on the salicylaldehyde moiety by coupling bromo-salicylaldehyde **2** with tert-butylacetylene **3** to yield **4**, which was reacted with 4-bromo-diaminobenzene **5** to obtain the salphen ligand **6**. Platinum was then coordinated using  $K_2PtCl_4$  as a source of Pt(II) to yield complex **7**. The alkyne spacer was introduced by a Sonogashira coupling reaction with trimethylsilylacetylene (TMSA) followed by deprotection to yield complex **9**. In a final step, **9** was connected to the terpyridine ligand by a double Sonogashira coupling reaction with dibromoterpyridine **10** to afford tweezers **1** in 83 % yield. Despite its rather low solubility, **1** was characterised by NMR and mass spectrometry. The 2D NOESY spectrum in DMSO and THF were consistent with a 'W' shaped geometry of the terpyridine ligand with the absence of correlation between protons H-2 and H-3 (see Fig S17 in the ESI), as expected from the electronic repulsion between the nitrogen lone pairs favouring the *s-trans* conformation.



Scheme 1. Synthesis of molecular tweezers **1**.

### Switching studies

Closing of the tweezers was monitored by UV-Vis spectroscopy. Titration of **1** with zinc(II) perchlorate (Fig 2) showed a single step evolution up to 1 eq with a bathochromic shift of the band corresponding to the absorption of the Pt-salphen moiety and of the terpyridine unit. Isosbestic points were observed at all curve crossings ( $\lambda = 580, 510, 498, 454, 398, 381, 364$  and  $349$  nm), which is consistent with an

equilibrium solely between the open and closed form. The formation of a potential Zn-bis(terpy) intermediate  $[Zn(1)_2]^{2+}$  reported in the literature with simple terpyridine ligands was not observed.<sup>17</sup> The 1:1 stoichiometry of the obtained complex was also confirmed by a Job plot showing a maximum at 0.5 (see Fig S20 in ESI). Curve fitting revealed a strong association constant ( $\log K_{\text{ass}} = 7$ ) affording total closing at around 1 eq of cation. A titration and Job plot was also performed with  $ZnCl_2$  (see Fig S21 and S22 in ESI) showing the same behaviour and a slightly higher association constant ( $\log K_{\text{ass}} = 7.3$ ). The  $^1H$ -NMR spectrum in THF- $d_8$  (Fig 3) is characteristic of a coordinated terpy ligand with downfield shifts for para-protons H-1 and H-4 compared to the open tweezers. Large shifts are also observed for the protons of the Pt-salphen moieties. In particular, proton H-6 is strongly deshielded while H-7 is subject to an upfield shift, due to the magnetic anisotropy effects of the stacked aromatic rings in the "U" conformation. These large changes in the spectra are consistent with the proposed mechanical motion induced by the coordination of the terpy ligand. Finally, single crystals suitable for X-ray diffraction were obtained by vapour diffusion, confirming the structure of the closed tweezers (Fig 4).

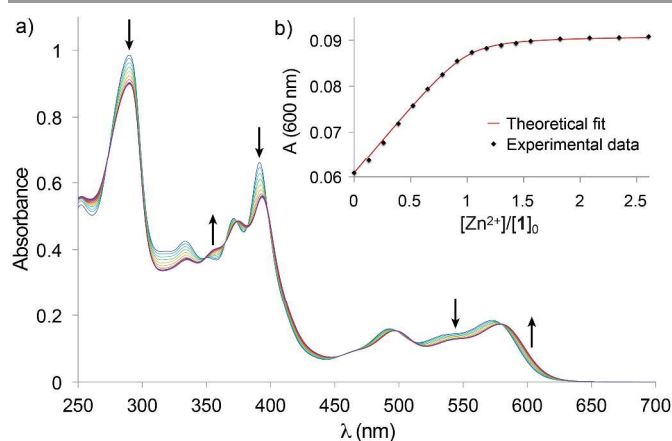


Fig 2. a) UV-Vis titration of **1** ( $5.0 \times 10^{-6}$  mol·L<sup>-1</sup>) by  $Zn(ClO_4)_2$  in THF. b) Absorption at 600 nm and fitting with a 1:1 binding model.

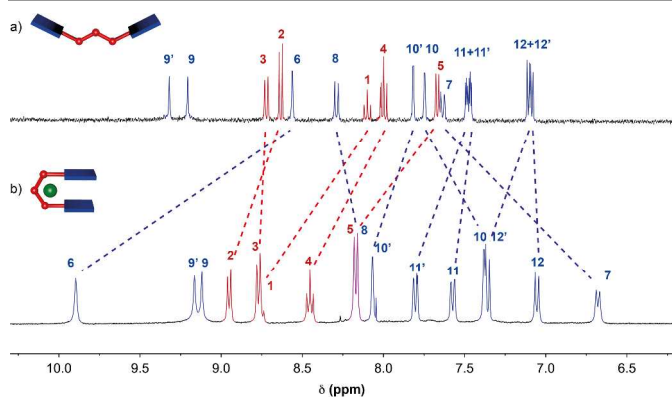


Fig 3.  $^1H$  NMR spectra (400 MHz, 300 K) in THF- $d_8$  of a) tweezers **1** and b)  $[Zn(1)Cl_2]$ .

The closed tweezers  $[\text{Zn}(\mathbf{1})]\text{Cl}_2$  crystallized in a triclinic space group (P-1) with one molecule in the asymmetric unit in a rather compact unit cell ( $a = 15.2042(4)$ ,  $b = 17.3084(4)$ ,  $c = 17.7406(4)$  Å,  $\alpha = 65.543(2)$ ,  $\beta = 89.942(2)$ ,  $\gamma = 88.527(2)^\circ$ ,  $V = 4248.08(19)$  Å<sup>3</sup>). The  $\text{Zn}^{2+}$  is bound to the terpyridine N atoms and two chloride ligands in a distorted trigonal bipyramidal geometry (Fig 4a-b). Each platinum atom displays a square planar geometry with average Pt–N and Pt–O distances of 1.95(1) and 1.99(1) Å, respectively, which are similar to those previously reported for Pt-salphen complexes.<sup>18</sup> The terpyridine ligand adopts a twisted geometry resulting in a folded helical structure with the two arms crossing at the level of the salphen unit with an almost 90° angle (Fig 4b). The two helical enantiomers *P* and *M* are present in the unit cell, revealing no spontaneous resolution upon crystallization. This folded conformation allows the stacking of the Pt-salphen moieties with an average intramolecular interplanar separation (defined as the Pt-to-Pt(N<sub>2</sub>O<sub>2</sub>) plane distance) of 3.32 Å. This distance, which is shorter than in most of the Pt-salphen described in the literature (~3.4 Å),<sup>18</sup> and the almost parallel orientation (average angle of 2.9°) between the two units reveal a strong  $\pi$ -stacking interaction enabled by the remote position of the *tert*-butyl groups. The near coplanarity between the salphen and terpyridine (14° dihedral angle) allows an extended electronic delocalization of the  $\pi$ -system via the triple bond and provides additional stabilization. Moreover, the two salphen units are almost superposed resulting in an intramolecular Pt–Pt distance of 3.481(1) Å, which is at the upper limit of typical Pt–Pt bond (2.7 Å <  $d$  < 3.5 Å).<sup>19</sup> However a much shorter intermolecular Pt–Pt bond of 3.212(1) Å is observed in the crystal structure (Fig 4c) with a head to tail arrangement between the two salphen units in the dimer. Such strong stacking associated with Pt–Pt bond was not observed in the previously studied tweezers showing the interest of this new design to increase the accessibility of the salphen units.

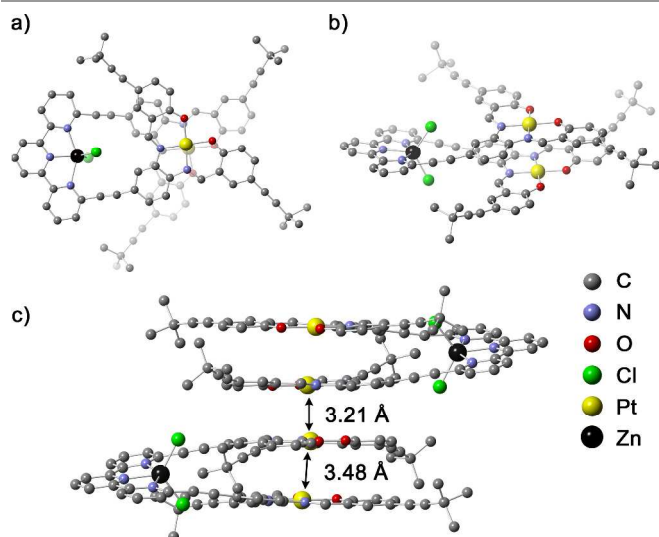


Fig 4. Single crystal X-ray diffraction structure of  $[\text{Zn}(\mathbf{1})]\text{Cl}_2$  a) top and b) side view; c) packing diagram showing intramolecular and intermolecular Pt–Pt bond distances (bottom). Solvent molecules and hydrogen atoms are omitted for clarity.

This crystal structure also alludes to the non-formation of the intermediate  $[\text{Zn}(\mathbf{1})_2]^{2+}$  complex during the titration. Indeed, the strong intramolecular stacking of the Pt-salphen moieties might confer high stability to the 1:1 complex, thus preventing the coordination of a second terpyridine ligand in an orthogonal position.

The closed tweezers can be reopened by addition of a competitive ligand having a higher complexation constant than the terpyridine. Tris 2-aminoethyl amine (tren) was chosen due to its high binding constant with metallic cations.<sup>20</sup> The reopening of the tweezers closed with  $\text{Zn}^{2+}$  was investigated by UV-Vis titration (Fig 5). A complete reopening of  $[\text{Zn}(\mathbf{1})]^{2+}$  was observed after addition of around 2 eq of tren. The presence of isosbestic points at all curve crossings ( $\lambda = 580$ , 510, 498, 454, 398, 376, 364 and 349 nm) is consistent with only two absorbing species in equilibrium. The reopening follows the reverse path of the closing with no evidence of an intermediate  $[\text{Zn}(\mathbf{1})_2]^{2+}$  complex. This demonstrates the reversible working operation of the tweezers that can be closed and reopened depending on the stimuli used, similarly to the tweezers that we reported earlier.<sup>16</sup>

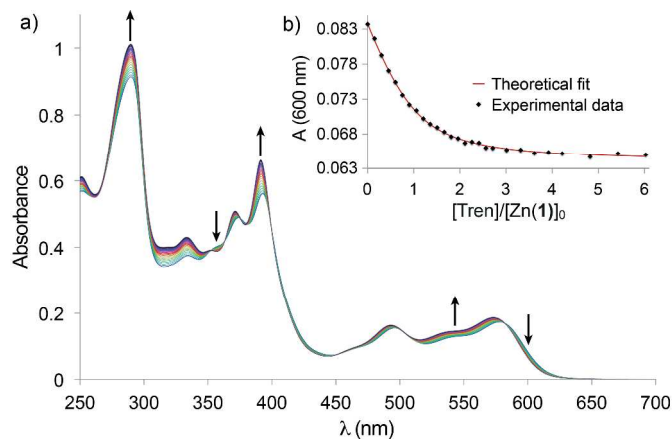


Fig 5. a) UV-Vis titration of  $[\text{Zn}(\mathbf{1})]^{2+}$  ( $5.0 \times 10^{-6}$  mol·L<sup>-1</sup>) upon addition of Tren in THF, after closing with 1 equivalent of  $\text{Zn}(\text{ClO}_4)_2$ . b) Absorption at 600 nm and fitting with a 1:1 binding model.

### Intercalation studies

The recognition and intercalation abilities of closed tweezers  $[\text{Zn}(\mathbf{1})]^{2+}$  towards flat aromatic molecules were investigated in analogy with bis(Pt-terpy) molecular clips reported in the literature.<sup>14a, 14b</sup> However the addition of aromatic compounds of various sizes and electronic properties (anthracene, pyrene, perylene, coronene, trinitrofluorenone) to  $[\text{Zn}(\mathbf{1})]^{2+}$ , resulted in no clear evidence of intercalation by UV-Vis titration. Even the addition of a Pt-salphen complex where a Pt–Pt interaction should be an additional driving force<sup>14c, 14d</sup> did not result in any intercalation. These disappointing results might be explained by the flexibility of the alkyne spacers between the terpy and the salen units that allows a folded geometry and a strong stacking between the Pt-salphen, as observed in the crystal structure, thus preventing the intercalation of a substrate. This intramolecular stacking is also entropically-favoured compared

to intermolecular interaction with substrates. Substrates with a metal binding capacity such as 2,2'-bipyridine (bipy) and 1,10-phenanthroline (phen) were also tested to potentially complete the coordination sphere of the zinc and stack with the phenylene moiety of the Pt-salphen. UV-Vis titration with bipy showed no sign of intercalation, however with phen isosbestic points ( $\lambda = 581, 500, 455, 399, 380$  and  $365$  nm) were obtained during the addition of up to 10 eq (see Fig S25 in ESI). The evolution is similar to the one observed with tren indicating a gradual reopening of the tweezers. In this case a larger excess of phen ligand is necessary to effect this change due to its lower binding constant.<sup>21</sup>

Inspired by the described interaction of  $\text{Pb}^{2+}$  with Pt-salen clips<sup>15</sup> and our previous work,<sup>16</sup> the effect of  $\text{Pb}^{2+}$  and  $\text{Hg}^{2+}$  were investigated by UV-Vis spectroscopy. Titration with  $\text{Pb}(\text{ClO}_4)_2$  (see Fig S23 in ESI) presented a similar behaviour as  $\text{Zn}^{2+}$  with a single evolution up to 1 eq and isosbestic points corresponding to the coordination to the terpyridine moiety ( $\log K_{\text{ass}} = 7$ ). A Job plot confirmed the formation of 1:1 complex  $[\text{Pb}(\mathbf{1})]^{2+}$  (see Fig. S24 in ESI).

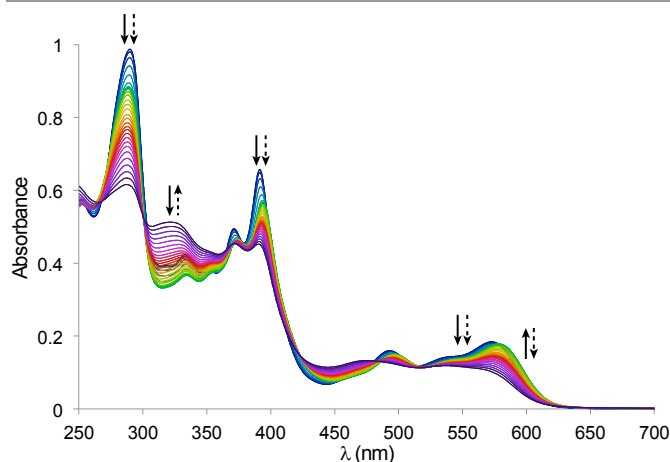


Fig 6. UV-Vis titration of Tweezers **1** ( $5.0 \times 10^{-6}$  mol·L<sup>-1</sup>) by  $\text{Hg}(\text{ClO}_4)_2$  in THF at 298 K (Bold arrows: first evolution 0 to 1 eq; dashed arrows: second evolution 1 to 10 eq).

However,  $\text{Hg}^{2+}$  presented a particular behaviour with a double evolution (Fig 6). Up to around 1 eq the system behaves as with other metals, with a bathochromic shift of the low energy absorption band of the Pt-salphen unit to 578 nm and a decrease of the 390 nm band characteristic of the terpyridine coordination and closed tweezers form. However, upon addition of more than one equivalent of mercury ion another evolution was observed with the appearance of new isosbestic points (see Fig S27-28) and a dramatic change in the absorption spectrum that can be attributed to the interaction with a second  $\text{Hg}^{2+}$  as observed with our structurally-related tweezers.<sup>16</sup> Since Job's method becomes unreliable when there is more than one complex present in competitive equilibrium,<sup>22</sup> the titration isotherm with  $\text{Hg}^{2+}$  was treated by a non-linear fit of the titration data.<sup>22c</sup> The UV-Vis data were fitted, with good agreement, using a 1:2 (host: guest) binding model (see Fig S29 in the ESI) demonstrating the formation of a new  $[\text{Hg}_2(\mathbf{1})]^{4+}$

species. This new species was also studied by mass spectrometry by adding  $\text{Hg}(\text{ClO}_4)_2$  to a solution of closed  $[\text{Hg}(\mathbf{1})\text{Cl}_2]$  tweezers. The characteristic signal of doubly charged  $[\text{Hg}_2(\mathbf{1})\text{Cl}_2]^{2+}$  at  $1044.6$   $m/z$  and mono charged  $[\text{Hg}_2(\mathbf{1})\text{Cl}_2(\text{ClO}_4)]^+$  at  $2188.2$   $m/z$  were observed in ESI-TOF confirming the formation a species with two  $\text{Hg}^{2+}$  (see Fig S30-31 in ESI).

Since single crystals of suitable quality for diffraction studies could not be obtained, DFT calculations (B3LYP/6-31G\*\*/LanL2dz) were performed in order to assess the location of the second mercury ion. An optimized structure was obtained showing the tweezers in a folded geometry similar to the one in the crystal structure but with the two Pt-salphen units adopting a *syn* conformation. The first  $\text{Hg}^{2+}$  ion is coordinated to the terpy ligand and the second one to the four oxygen atoms of the salphen units and bound by a bidentate perchlorate ligand (Fig 7). This hexacoordinated mercury(II) ion adopts a distorted octahedral geometry similar to that described previously for rigid Pt-salphen clips with  $\text{Pb}^{2+}$ .<sup>15b</sup> The average Hg-O bond distance (2.45 Å) is, however, slightly shorter than those reported in crystallographic structures of  $\text{Hg}^{2+}$  coordinated to the oxygen salen complexes.<sup>23</sup>

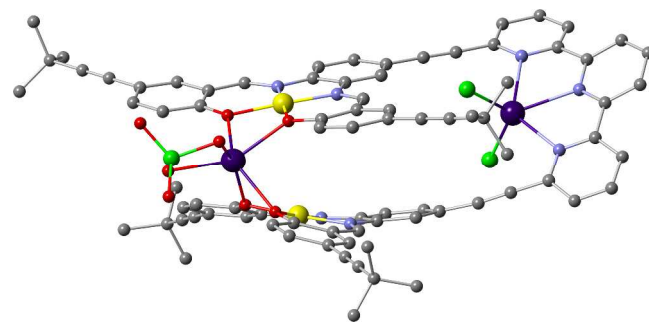


Fig 7. DFT optimized structure of  $[\text{Hg}(\text{ClO}_4)_2 @ \text{HgCl}_2(\mathbf{1})]^+$ . Hydrogen atoms are omitted for clarity.

As observed with  $\text{Zn}^{2+}$  and  $\text{Pb}^{2+}$ , a reversible reopening of  $[\text{Hg} @ \text{Hg}(\mathbf{1})]^{4+}$  was also obtained by addition of tren. Therefore the tweezers represent a reversible allosteric system: closing by metal coordination leads to the formation of a new binding site able to selectively host mercury. The mechanical motion can be harvested to generate positive cooperativity with selective binding and release of a mercury(II) cation.

### Photophysical properties

The photophysical properties of tweezers **1** and the effect of closing were investigated by UV-Vis absorption and emission spectroscopy (Table 1). The photophysical measurements were performed at low concentration ( $5 \times 10^{-6}$  mol·L<sup>-1</sup>) in order to avoid aggregation and to record spectra free of artifacts arising from measurements of high optical density solutions. The UV-Vis absorption spectra of **1** in THF comprises bands at  $\lambda < 400$  nm ( $\epsilon > 1 \times 10^5$  L·mol<sup>-1</sup>·cm<sup>-1</sup>) and less intense absorption bands in the visible region ( $\lambda_{\text{max}} = 573$  nm;  $\epsilon = 37 \times 10^3$  L·mol<sup>-1</sup>·cm<sup>-1</sup>). The same features are found for closed tweezers  $[\text{Zn}(\mathbf{1})]^{2+}$ ,  $[\text{Pb}(\mathbf{1})]^{2+}$  and  $[\text{Hg}(\mathbf{1})]^{2+}$  with a slight

bathochromic shift of 6 nm for the low energy transition. By comparison with the literature, the UV absorption bands can be assigned to intraligand ( $\pi-\pi^*$ ) transitions of the salphen and terpy, whereas the low-energy absorption bands between 480 and 580 nm can be attributed to O(p)/Pt(d) $\rightarrow\pi^*$  (diimine) charge-transfer transitions.<sup>24</sup> This assignment is supported by the solvatochromism observed for the absorption bands of [Zn(**1**)]<sup>2+</sup> and model complex **8** (see Fig S33 in ESI). The observed shift of band maxima to higher energy in solvents of increasing polarity (toluene, DCM, THF, dioxane to DMSO) is indicative of a polar ground state and a nonpolar excited state. Similar results have been previously observed for structurally-related Pt–Schiff base derivatives.<sup>24b, 25</sup>

Table 1. Photophysical data for tweezers **1** and complexes with Zn<sup>2+</sup>, Hg<sup>2+</sup> and Pb<sup>2+</sup> in THF at 298 K.

Compound	$\lambda_{abs}$ [nm] ( $\epsilon$ [L·mol <sup>-1</sup> ·cm <sup>-1</sup> ])	$\lambda_{em}$ [nm]	$\tau_{em}$ [μs]	$\Phi_{em}$
Tweezers <b>1</b>	391 (132 000) 573 (37 000)	659 613	3.9	0.16
[Zn( <b>1</b> )]Cl <sub>2</sub>	393 (109 000) 578 (34 400)	664 616	4.5	0.19
[Zn( <b>1</b> )](ClO <sub>4</sub> ) <sub>2</sub>	394 (111 000) 579 (34 600)	663 616	4.2	0.16
[Pb( <b>1</b> )](ClO <sub>4</sub> ) <sub>2</sub>	394 (112 000) 579 (34 200)	661 618	2.5	0.17
[Hg( <b>1</b> )](ClO <sub>4</sub> ) <sub>2</sub>	394 (113 000) 579 (35 200)	663 619	3.8	0.18
[Hg c Hg( <b>1</b> )] (ClO <sub>4</sub> ) <sub>4</sub> <sup>-</sup>	370 (88 600) 530 (22 800)	618	-	0.012

Luminescence properties were measured on degassed solutions at  $5.0 \times 10^{-6}$  mol·L<sup>-1</sup> ( $\lambda_{ex} = 532$ nm).

Tweezers **1** displays structured room temperature emission ( $\lambda_{max} = 659$  nm) in THF at 298 K, with a long emission lifetime ( $\tau = 3.9$  μs) indicating phosphorescence (Fig 8, see Table 1). The phosphorescence can be attributed to mixed triplet intraligand charge transfer and metal-to-ligand charge-transfer excited states.<sup>24</sup> The emission spectra recorded in 2-methyl tetrahydrofuran glasses at 77 K (see Fig S35 in ESI) present a vibronic progression ( $\sim 1500$  cm<sup>-1</sup>) characteristic of the ring stretching mode of the ligand and reveals the intraligand character of the emissive triplet excited state.<sup>25a</sup> Upon metal coordination the relative intensity of the emission band changes with a relative increase at the higher energy region of the emission band concomitant with a slight bathochromic shift with respect to the open tweezers **1** (Table 1). At first glance, it might be surprising to observe such small variations between open and closed forms. However, such small emission shifts have been observed for Pt-salphen clips by Chan et al<sup>15c</sup> where the proximity of two Pt units also resulted in small bathochromic shifts compared to the mononuclear complex. The emission quantum yield of the open form ( $\Phi_{em} = 0.16$ ) and lifetime slightly increase upon closing by Zn<sup>2+</sup> (Table 1). The emission of [Zn(**1**)]Cl<sub>2</sub> presented minor concentration dependence across the broad range 0.1 mM to 0.001 mM. Only a small (< 5%) change in the intensity of the first band was observed in the emission spectra, which were normalized with respect to the major band. This indicates the absence of

aggregation at the concentration ( $5 \times 10^{-6}$  mol·L<sup>-1</sup>) used during the photophysical studies and that the slight bathochromic shift observed upon closing might be due to weak  $\pi$ -stacking interactions between the two Pt-salphen units. The same shifts on the emission spectra are observed upon coordination of Pb<sup>2+</sup> or one Hg<sup>2+</sup> ion, with similar enhancement of luminescence compared to the open tweezers (compare entries 4 and 5 to entry 1 in Table 1). The emission lifetimes measured for the Pt-salphen moieties are not significantly affected by the tweezers closing, which is in accordance with the small modification in the quantum yields (Table 1). In all cases, no evidence of Pt-Pt interactions in the excited state was observed as such interactions may be anticipated to lead to a new, broad unstructured low energy emission band<sup>26</sup> that was not observed in our case. However, the intercalation of a second mercury ion results in a large decrease of the quantum yield ( $\Phi_{em} = 0.012$ ) associated with a differential quenching between the two emission bands. Compared to the open tweezers or closed with Hg<sup>2+</sup> (1 eq), the relative intensity of the two bands is inverted (see normalized emission Fig S32 in ESI). This quenching might be explained by the direct coordination of Hg<sup>2+</sup> to the emissive Pt-salphen moieties leading to new non-radiative deactivation pathway.

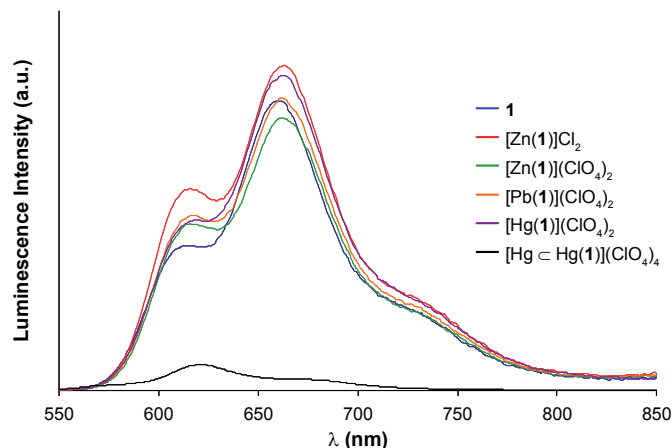


Fig 8. Emission of degassed solutions ( $5.0 \times 10^{-6}$  mol·L<sup>-1</sup>) in THF at 298 K ( $\lambda_{ex} = 532$  nm).

Surprisingly, emission of a single crystal of [Zn(**1**)]Cl<sub>2</sub> presented an unstructured emission at 664 nm (Fig 9). Compared to the solution spectra, the disappearance of the emission band at 616 nm was evidenced. Interestingly, this spectral change was also observed in a frozen matrix (see Fig S35 in ESI). Taken together, suppression of the blue-end emission band in these two cases may be associated with steric constraint, prohibiting structural reorganization/relaxation in the excited state. Furthermore, this effect may in turn affect the interaction of two close-lying states under thermal equilibrium at room temperature. This behavior, which has been observed for several chromophore pairs, would be consistent with the room temperature monoexponential luminescence decay and loss of the higher energy emission feature at low temperature.<sup>27</sup>

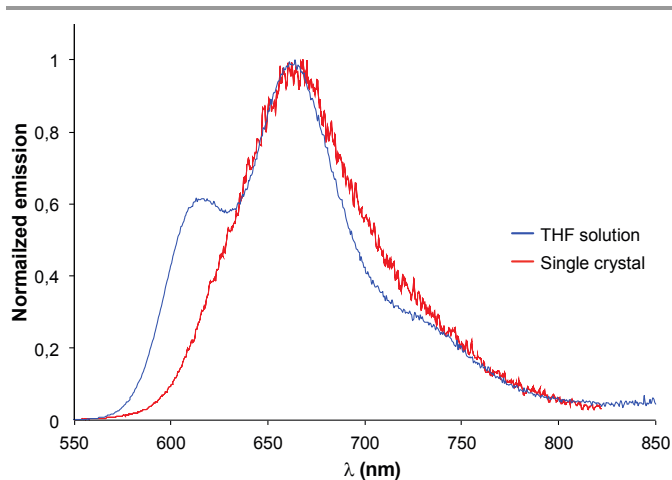


Fig 9 Emission of  $[Zn(1)]Cl_2$  in solution in THF ( $5.0 \times 10^{-6} \text{ mol}\cdot\text{L}^{-1}$ ) and in the crystal form ( $\lambda_{ex} = 532 \text{ nm}$ ).

## Conclusions

In conclusion, molecular tweezers based on a terpyridine bis Pt-salphen complex have been synthesized. The tweezers can be closed by coordination and reversibly re-opened by addition of the competitive tren ligand demonstrating a reversible operation of the system. Compared to previously studied tweezers, the remote position of the tert-butyl groups enabled a strong  $\pi$ -stacking between the salphen units in the closed form with intramolecular and intermolecular Pt-Pt bonds in the crystallographic structure. This strong stacking may have prevented intercalation of aromatic substrates but allowed a selective recognition of  $Hg^{2+}$  in the closed form. While the coordination of the terpy had little influence on the luminescence of the Pt-salphen moiety, the interaction with  $Hg^{2+}$  caused a large quenching associated with an inversion of the relative intensity of the structured emission. An unexpected loss of the structured emission was observed for single crystals of the zinc-closed tweezers that will be further investigated by TD-DFT calculations and reported in due course.

## Experimental section

**General Analytical and Synthetic Methods.**  $^1H$  NMR and  $^{13}C$  NMR spectra were recorded at 400 or 600 MHz on Bruker Avance III spectrometers. Chemical shifts ( $\delta$ ) are reported in ppm from tetramethylsilane using residual solvent peaks for calibration. Electrospray ionisation (ESI) mass spectrometry was performed on a Bruker microTOF spectrometer. Reagent grade tetrahydrofuran was distilled from sodium and benzophenone. Tetrahydrofuran and triethylamine were degassed by three freeze-pump-thaw cycles before being used in the Sonogashira coupling reactions. All others chemicals were purchased from commercial suppliers and used without further purification. Flash column chromatography was performed using silica gel from Merck (40-63  $\mu\text{m}$ ) or GraceResolv High Resolution Flash Cartridges (particle size 40  $\mu\text{m}$ ). Thin layer chromatography was performed using

aluminium plates pre-coated with silica gel 60 F254 0.20 mm layer thickness purchased from VWR. Absorption spectra were recorded on a JASCO V-670 spectrophotometer.

**Compound 4.** In a Schlenk tube under argon, 5-bromosalicylaldehyde **2** (1.0 g, 4.97 mmol, 1 eq),  $PdCl_2(PPh_3)_2$  (523 mg, 0.746 mmol, 15 mol%) and CuI (284 mg, 1.49 mmol, 30 mol%) were introduced. A mixture of  $NEt_3$  (10 mL) / THF (20 mL) previously distilled and degassed by freeze pump thaw was then added. 3,3-Dimethyl-1-butyne (1.22 mL, 9.94 mmol, 2 eq) was then added, and the mixture was heated at 70 °C under argon during 18 h. After solvent evaporation, the dark red solid was dissolved in dichloromethane and washed by an HCl solution (1M), then by water. The organic phase was dried over  $MgSO_4$ , filtered and evaporated. The crude dark solid was then purified by column chromatography ( $SiO_2$ : Cyclohexane / AcOEt - 0-8 %), yielding **4** as a white solid (860 mg, 86 %).  $^1H$  NMR: (400 MHz,  $CDCl_3$ )  $\delta$  11.01 (s, 1H), 9.85 (s, 1H), 7.61 (d,  $J = 2.1$  Hz, 1H), 7.53 (dd,  $J = 8.7, 2.1$  Hz, 1H), 6.91 (d,  $J = 8.7$  Hz, 1H), 1.31 (s, 9H);  $^{13}C$  NMR (100 MHz,  $CDCl_3$ )  $\delta$  196.30, 160.92, 140.11, 136.82, 120.51, 117.91, 116.22, 98.14, 31.15, 28.06; ESI-HRMS  $m/z$  (%):  $[M-H]^-$  calc ( $C_{13}H_{13}O_2$ ): 201.0921 (100), found: 201.0914 (100); Elemental analysis calc (%) for  $C_{13}H_{14}O_2$ : C 77.20, H 6.98, N 0; found: C 77.18, H 7.06, N 0.

**Compound 6.** In a round bottom flask were added 4-bromo-1,2-diaminobenzene **5** (347 mg, 1.86 mmol, 1 eq), **4** (788 mg, 3.90 mmol, 2.1 eq), and absolute ethanol (15 mL). After refluxing during 2 h, the mixture was put in the freezer during 15 h, then the resulting orange precipitate was filtered. After drying under vacuum, **6** was obtained as a yellow solid, with 69 % yield (715 mg).  $^1H$  NMR: (400 MHz,  $CDCl_3$ )  $\delta$  12.88 (s, 1H), 12.77 (s, 1H), 8.54 (s, 2H), 7.48 – 7.35 (m, 5H), 7.36 (d,  $J = 2.1$  Hz, 1H), 7.09 (d,  $J = 8.4$  Hz, 1H), 6.97 (d,  $J = 1.6$  Hz, 1H), 6.94 (d,  $J = 1.5$  Hz, 1H), 1.31 (s, 9H), 1.31 (s, 9H);  $^{13}C$  NMR: (100 MHz,  $CDCl_3$ )  $\delta$  164.06, 163.47, 160.87, 143.68, 141.60, 137.18, 137.03, 135.83, 135.63, 130.77, 122.89, 121.05, 121.01, 118.95, 118.85, 117.90, 115.25, 115.16, 97.41, 97.35, 78.06, 78.02, 31.24, 28.07; ESI-HRMS  $m/z$  (%):  $[M+H]^+$  calc ( $C_{32}H_{32}BrN_2O_2$ ): 557.1623 (100), found: 557.1628 (100); Elemental analysis calc (%) for  $C_{32}H_{31}BrN_2O_2$ : C 69.19, H 5.63, N 5.04; found: C 69.02, H 5.52, N 4.88.

**Complex 7.** In a Schlenk tube under argon were introduced **6** (600 mg, 1.08 mmol, 1 eq),  $K_2PtCl_4$  (493 mg, 1.19 mmol, 1.1 eq),  $K_2CO_3$  (448 mg, 3.24 mmol, 3 eq), and anhydrous DMSO previously degassed (15 mL). The mixture was heated at 80 °C during 16 h. After dilution with  $CH_2Cl_2$ , the organic phase was washed with pure water (three times), dried over  $MgSO_4$ , filtered, and evaporated. The crude product was purified by plug filtration ( $SiO_2$ :  $CH_2Cl_2$  / AcOEt - 0-3%), filtrate evaporation and drying yielded **7** as a dark pink solid (88 %, 712 mg).  $^1H$  NMR: (400 MHz,  $CDCl_3$ )  $\delta$  8.21 (s, 1H), 8.16 (s, 1H), 7.55 (d,  $J = 2.0$  Hz, 1H), 7.45 – 7.30 (m, 4H), 7.15 (d,  $J = 2.2$  Hz, 1H), 7.04 (dd,  $J = 8.7, 1.8$  Hz, 1H), 7.00 (d,  $J = 8.9$  Hz, 1H), 6.91 (d,  $J = 8.9$  Hz, 1H), 1.35 (s, 2H);  $^{13}C$  NMR (101 MHz,  $CDCl_3$ )  $\delta$  165.21, 164.79, 148.14, 147.99, 145.37, 143.57, 138.72, 138.59, 137.81, 137.52, 130.00, 122.71,

122.41, 121.23, 121.19, 121.07, 118.22, 115.92, 112.80, 112.65, 97.18, 97.10, 78.11, 78.05, 31.48, 31.43, 28.11; ESI-HRMS  $m/z$  (%):  $[M+Na]^+$  calc ( $C_{32}H_{29}BrN_2O_2PtNa$ ): 771.0918 (100), found: 771.0947 (100); Elemental analysis calc (%) for  $C_{32}H_{29}BrN_2O_2Pt$ : C 51.34, H 3.90, N 3.74; found: C 51.63, H 4.40, N 3.68.

**Complex 8.** In a Schlenk tube under argon were introduced **7** (500 mg, 0.668 mmol, 1 eq),  $PdCl_2(PPh_3)_2$  (70 mg, 0.100 mmol, 15 mol%),  $CuI$  (38 mg, 0.200 mmol, 30 mol%). A mixture of  $NEt_3$  (10 mL) / THF (20 mL) previously distilled and degassed was then added. TMSA (0.76 mL, 5.34 mmol, 8 eq) was added and the mixture was then stirred under argon at 70°C during 16 h. Solvent was evaporated under reduced pressure and the crude product was purified by column chromatography ( $SiO_2$ : Cyclohexane /  $CH_2Cl_2$  / AcOEt, 100/0/0 – 0/100/0 – 0/96/4, v/v/v) yielding 92 % (468 mg) of **8** as a dark pink solid.  $^1H$  NMR: (400 MHz,  $CDCl_3$ )  $\delta$  8.49 (s, 1H), 8.48 (s, 1H), 7.74 (d,  $J = 1.5$  Hz, 1H), 7.68 (d,  $J = 8.7$  Hz, 1H), 7.52 (d,  $J = 2.2$  Hz, 1H), 7.49 – 7.44 (m, 4H), 7.39 (d,  $J = 2.3$  Hz, 1H), 7.22 (dd,  $J = 8.6, 1.5$  Hz, 1H), 7.15 (d,  $J = 8.9$  Hz, 1H), 7.12 (d,  $J = 8.9$  Hz, 1H), 1.34 (s, 9H), 1.34 (s, 9H), 0.33 (s, 9H);  $^{13}C$  NMR (101 MHz,  $CDCl_3$ )  $\delta$  165.14, 165.06, 148.32, 148.26, 144.45, 144.34, 138.69, 138.63, 137.72, 137.53, 130.77, 122.75, 122.66, 122.52, 121.40, 118.61, 115.28, 112.70, 112.67, 103.15, 97.29, 97.05, 97.03, 78.23, 78.17, 31.45, 31.43, 28.09, 0.17; ESI-HRMS  $m/z$  (%):  $[M+Na]^+$  calc ( $C_{37}H_{38}N_2O_2PtSiNa$ ): 788.2245 (100), found: 788.2235 (100); Elemental analysis calc (%) for  $C_{37}H_{38}N_2O_2PtSi$ : C 58.02, H 5.00, N 3.66; found: C 58.18, H 5.28, N 3.34.

**Complex 9.** To complex **8** (375 mg, 0.490 mmol, 1eq) in a round bottom flask, were successively added  $K_2CO_3$  (135 mg, 0.979 mmol, 2eq), THF (10 mL), and MeOH (10 mL). The mixture was stirred at room temperature during 90 min. After solvent evaporation under reduced pressure, the red solid was purified by plug filtration ( $Al_2O_3$ :  $CH_2Cl_2$  / MeOH, 10 %). The filtrate was evaporated yielding 93 % (316 mg) of **9** as a red solid.  $^1H$  NMR: (400 MHz,  $CDCl_3$ )  $\delta$  8.57 (s, 1H), 8.56 (s, 1H), 7.87 (s, 1H), 7.75 (d,  $J = 8.7$  Hz, 1H), 7.56 – 7.47 (m, 4H), 7.30 – 7.27 (m, 1H), 7.21 – 7.16 (m, 2H), 3.22 (s, 1H), 1.34 (s, 18H); The material was not sufficiently soluble for  $^{13}C$  analysis; ESI-HRMS  $m/z$  (%):  $[M+Na]^+$  calc ( $C_{34}H_{30}N_2O_2PtNa$ ): 716.1850 (100), found: 716.1863 (100); Elemental analysis calc (%) for  $C_{34}H_{30}N_2O_2Pt$ : C 58.87, H 4.36, N 4.04; found: C 58.46, H 4.85, N 3.47.

**Tweezers 1.** In a Schlenk tube under argon were introduced 6,6''-dibromo-2,2':6',2''-terpyridine **10** (14 mg, 0.036 mmol, 1eq), **9** (100 mg, 0.144 mmol, 4 eq),  $PdCl_2(PPh_3)_2$  (5 mg, 0.0072 mmol, 20 mol%),  $CuI$  (3 mg, 0.014 mmol, 40 mol%). A mixture of  $NEt_3$  (4 mL) / THF (8 mL) previously distilled and degassed was then added. The mixture was stirred at 70°C under argon during 15 h. After solvent evaporation, chloroform, and 10 drops of tris(2-aminoethyl)amine were added. The mixture was then washed with water ( $3 \times 50$  mL), the organic phase was dried over  $MgSO_4$ . The organic phase was filtered and the  $MgSO_4$  thoroughly washed with hot THF. After solvent evaporation the crude product was recrystallized from

chloroform yielding 48 mg (83 %) of **1** as a dark pink solid. Note: Treatment with excess tris(2-aminoethyl)amine during purification was performed in order to remove any remaining Cu or Pd from the Sonogashira coupling reaction. Mass spectrum showed no additional peak of coordinated tweezers and 2D NOESY spectra in THF or DMSO are consistent with an open form with no correlation peak between protons H-2 and H-3 of the terpy (see Fig S17).  $^1H$  NMR: (400 MHz, DMSO- $d_6$ , 370K)  $\delta$  9.59 (s, 2H), 9.48 (s, 2H), 8.75 (s, 2H), 8.65 (d,  $J = 8.0$  Hz, 2H), 8.52 (d,  $J = 7.9$  Hz, 2H), 8.47 (d,  $J = 8.8$  Hz, 2H), 8.21 (t,  $J = 7.9$  Hz, 1H), 8.12 (t,  $J = 7.8$  Hz, 2H), 8.01 (d,  $J = 2.3$  Hz, 2H), 7.98 (d,  $J = 2.4$  Hz, 2H), 7.80 (d,  $J = 7.0$  Hz, 2H), 7.73 (dd,  $J = 8.7, 1.6$  Hz, 2H), 7.52 – 7.49 (m, 4H), 7.09 (d,  $J = 8.7$  Hz, 4H), 1.36 (s, 9H), 1.35 (s, 9H). The material was not sufficiently soluble for  $^{13}C$  analysis; ESI-HRMS  $m/z$  (%):  $[M+Na]^+$  calc ( $C_{83}H_{67}N_7O_4Pt_2Na$ ): 1638.4448 (100), found: 1638.4377 (100);

**Crystal data for [Zn(1)]Cl<sub>2</sub>.** Single crystals were grown by slow vapour diffusion of acetonitrile into a solution of [Zn(1)]Cl<sub>2</sub> in THF. Red plate-like crystals were obtained:  $C_{90}H_{76.50}Cl_2N_{10.5}O_4Pt_2Zn$ , triclinic, *P*-1,  $a = 15.2042(4)$ ,  $b = 17.3084(4)$ ,  $c = 17.7406(4)$  Å,  $\alpha = 65.543(2)$ ,  $\beta = 89.942(2)$ ,  $\gamma = 88.527(2)^\circ$ ,  $V = 4248.08(19)$  Å<sup>3</sup>,  $Z = 2$ ,  $T = 100(2)$  K,  $\mu = 3.125$  mm<sup>-1</sup>, 38348 reflections measured, 19740 observed [ $I \geq 2s(I)$ ], 1014 parameters, final R indices  $R_1$  [ $I \geq 2s(I)$ ] = 0.0919 and  $wR_2$  (all data) = 0.2550, GOF on  $F^2 = 1.028$ , max/min residual electron density = 5.25/-3.91 e<sup>-</sup>Å<sup>-3</sup>. CCDC 1027603 contains the supplementary crystallographic data for this paper. These data can be obtained free of charge from The Cambridge Crystallographic Data Centre via [www.ccdc.cam.ac.uk/data\\_request/cif](http://www.ccdc.cam.ac.uk/data_request/cif).

A single crystal of the compound was selected in a drop of glue, mounted onto a glass fiber, and transferred in a cold nitrogen gas stream. The data collection for [Zn(1)]Cl<sub>2</sub> was carried out on the 4-circle diffractometer at the CRISTAL beamline (SOLEIL synchrotron, Paris) using the synchrotron radiation source ( $\lambda = 0.66825$  Å) up to a maximum resolution of 0.8 Å<sup>-1</sup>, reaching 97 % of completeness. Data collection strategies were generated with the CrysAlisPro CCD package. Unit-cell parameters refinement, data reduction, scaling and absorption correction were carried out with CrysAlisPro. The sample was treated as a two domains twin for data reduction. In the WinGX suite of programs,<sup>28</sup> the structure was solved with SHELXS-97 program<sup>29</sup> and refined by full-matrix least-squares methods using SHELXL-2013 and a HKLF5 type hkl file. All non-hydrogen atoms were refined anisotropically while one acetonitrile solvent molecule was refined isotropically. Hydrogen atoms were placed at calculated positions. Geometrical restraints were introduced for tert-butyl groups and solvent molecules. Restraints on ADPs were also used for the latter parts of the structure.

**Switching studies:** UV-Vis titrations were performed using distilled THF by successive additions of aliquots of metal perchlorate solution (1.0 mM in THF, 0.1 equivalent  $\leftrightarrow$  1.5  $\mu$ L), to a 3.0 mL tweezers **1** solution (5.0  $\mu$ M in THF). Binding constants were obtained by a nonlinear least-squares fit of the

absorbance versus the concentration of guest added using the Matlab program developed by P. Thordarson.<sup>22c</sup>

**Photophysical studies:** Solutions for spectroscopic studies were degassed ( $9 \times 10^{-6}$  bar) by multiple freeze-pump-thaw cycles and the cell was blowtorch sealed. Electronic absorption spectra were recorded on dilute solutions ( $5.0 \times 10^{-6}$  mol·L<sup>-1</sup>) in 1 cm quartz cells using a Varian Cary-50 spectrometer. Steady-state luminescence spectra were recorded on a Horiba Jobin-Yvon Fluorolog-3 spectrofluorometer equipped with a R928P PMT and were corrected. Quantum yields ( $\Phi$ ) of complexes were determined on comparison with an optically dilute [Ru(bpy)<sub>3</sub>]Cl<sub>2</sub>, bpy = 2,2'-bipyridine, standard ( $\Phi_r$ ) in air-equilibrated water ( $\Phi_{em} = 0.042$  according to the equation:  $\Phi = \Phi_r(I/I_r)(A_r/A)(\eta^2/\eta_r^2)$ , where r refers to the reference, I is the integrated emission intensity, A is the absorbance at the excitation wavelength and  $\eta$  is the refractive index of the solvent. Luminescence lifetimes were measured via time-correlated single photon counting spectrometry on the spectrofluorometer, exciting with a 560 nm NanoLED (FWHM = ca. 1 ns). Emission of the single crystal was recorded on a previously described confocal fluorescence microscope setup.<sup>26</sup>

**Computational details:** Calculations were performed with the Gaussian 09 software.<sup>30</sup> Complete geometry optimizations were carried out using the density functional theory method with the conventional Becke-3-Lee-Yang-Parr (B3LYP) exchange-correlation functional and 6-31G\*\*/LanL2DZ. The platinum and mercury atoms were modelled using the effective core potential and the corresponding valence orbitals LanL2DZ in order to decrease the number of basis functions. The other atoms were described by the double zeta 6-31G\*\* base which takes into account the polarization orbitals of all atoms, including hydrogens. Vibrational analysis was performed at the same level in order to check the obtention of a minimum on the potential energy surface.

## Acknowledgements

B.D. thanks the Ecole Normale Supérieure of Cachan for a PhD Fellowship. Dr. Valérie Marvaud is warmly acknowledged for fruitful discussions. The authors acknowledge financial support from the University of Bordeaux and Région Aquitaine. This study has been carried out in the framework of the "Investments for the future" Programme LabEx MiChem ANR-11-IDEX-0004-02 and IdEx Bordeaux – LAPHIA (ANR-10-IDEX-03-02). We thank André Del Guerzo and Guillaume Raffy for assistance in recording the confocal fluorescence spectrum. We are grateful to Dr. P. Fertey (CRISTAL beamline team, synchrotron SOLEIL) and Dr. S. Pillet (CRM2, Nancy) for their kind help in the collection of SC-XRD data.

## Notes and references

<sup>a</sup> Sorbonne Universités, UPMC Univ Paris 06, UMR 8232, Institut Parisien de Chimie Moléculaire, 4 place Jussieu, 75005, Paris, France  
E-mail: [bernold.hasenknopf@upmc.fr](mailto:bernold.hasenknopf@upmc.fr), [guillaume.vives@upmc.fr](mailto:guillaume.vives@upmc.fr)

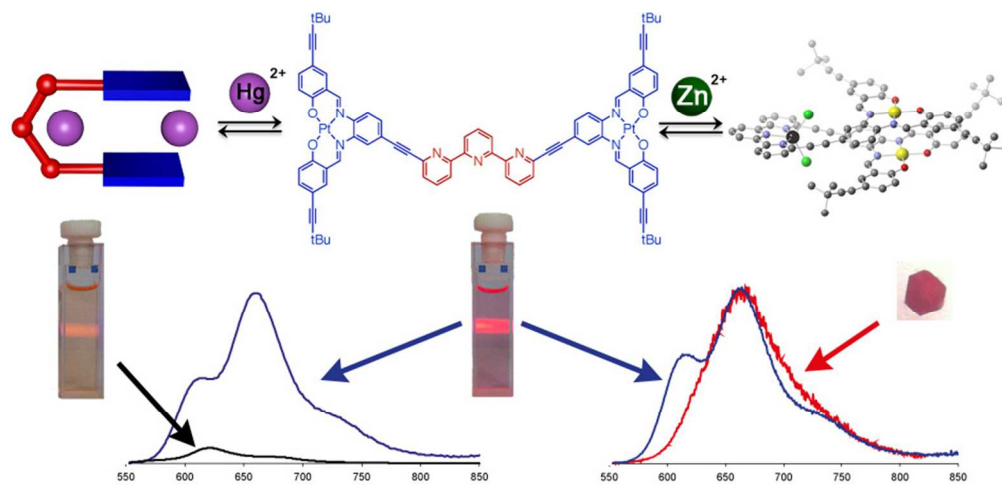
<sup>b</sup> CNRS, UMR 8232, Institut Parisien de Chimie Moléculaire, 4 place Jussieu, 75005, Paris, France.

<sup>c</sup> Univ. Bordeaux, ISM (CNRS UMR 5255), F-33400 Talence, France.

Electronic Supplementary Information (ESI) available: the supplementary information contains <sup>1</sup>H, <sup>13</sup>C NMR, UV-Vis titration data. See DOI: 10.1039/b000000x/

1. B. L. Feringa, *Molecular Switches*, Wiley-VCH, Weinheim, 2001.
2. V. Balzani, M. Venturi and A. Credi, *Molecular Devices and Machines: Concepts and Perspectives for the Nanoworld*, Wiley-VCH: Weinheim, 2008.
3. (a) T. R. Kelly, H. De Silva and R. A. Silva, *Nature*, 1999, **401**, 150-152; (b) N. Koumura, R. W. J. Zijlstra, R. A. Van Delden, N. Harada and B. L. Feringa, *Nature*, 1999, **401**, 152-155; (c) D. A. Leigh, J. K. Y. Wong, F. Dehez and F. Zerbetto, *Nature*, 2003, **424**, 174-179; (d) R. A. van Delden, M. K. J. ter Wiel, M. M. Pollard, J. Vicario, N. Koumura and B. L. Feringa, *Nature*, 2005, **437**, 1337-1340; (e) V. Balzani, M. Clemente-Leon, A. Credi, B. Ferrer, M. Venturi, A. H. Flood and J. F. Stoddart, *Proc. Natl. Acad. Sci. U. S. A.*, 2006, **103**, 1178-1183; (f) G. Vives, H. P. J. de Rouville, A. Carella, J. P. Launay and G. Rapenne, *Chem. Soc. Rev.*, 2009, **38**, 1551-1561; (g) U. G. E. Perera, F. Ample, H. Kersell, Y. Zhang, G. Vives, J. Echeverria, M. Grisolia, G. Rapenne, C. Joachim and S. W. Hla, *Nature Nanotech.*, 2013, **8**, 46-51.
4. (a) F. Puntoriero, F. Nastasi, T. Bura, R. Ziessel, S. Campagna and A. Giannetto, *New J. Chem.*, 2011, **35**, 948-952; (b) T. Gunnlaugsson and J. P. Leonard, *Chem. Commun.*, 2005, 3114-3131.
5. (a) N. Armaroli, V. Balzani, J. P. Collin, P. Gavina, J. P. Sauvage and B. Ventura, *J. Am. Chem. Soc.*, 1999, **121**, 4397-4408; (b) A. M. Brouwer, C. Frochot, F. G. Gatti, D. A. Leigh, L. Mottier, F. Paolucci, S. Roffia and G. W. H. Wurpel, *Science*, 2001, **291**, 2124-2128.
6. (a) T. C. Bedard and J. S. Moore, *J. Am. Chem. Soc.*, 1995, **117**, 10662-10671; (b) T. Lang, A. Guenet, E. Graf, N. Kyritsakas and M. W. Hosseini, *Chem. Commun.*, 2010, **46**, 3508-3510; (c) T. Lang, E. Graf, N. Kyritsakas and M. W. Hosseini, *Chem. Eur. J.*, 2012, **18**, 10419-10426; (d) N. Zigon, A. Guenet, E. Graf and M. W. Hosseini, *Chem. Commun.*, 2013, **49**, 3637-3639; (e) N. Zigon, N. Kyritsakas and M. W. Hosseini, *Dalton Trans.*, 2014, **43**, 152-157.
7. (a) Y. Shirai, J.-F. Morin, T. Sasaki, J. M. Guerrero and J. M. Tour, *Chem. Soc. Rev.*, 2006, **35**, 1043-1055; (b) G. Vives and J. M. Tour, *Acc. Chem. Res.*, 2009, **42**, 473-487; (c) T. Kudernac, N. Ruangsupapichat, M. Parschau, B. Macia, N. Katsonis, S. R. Harutyunyan, K. H. Ernst and B. L. Feringa, *Nature*, 2011, **479**, 208-211.
8. (a) J. Leblond and A. Petitjean, *ChemPhysChem*, 2011, **12**, 1043-1051; (b) M. Hardouin-Lerouge, P. Hudhomme and M. Salle, *Chem. Soc. Rev.*, 2011, **40**, 30-43; (c) F.-G. Klärner and B. Kahlert, *Acc. Chem. Res.*, 2003, **36**, 919-932.
9. C. W. Chen and H. W. Whitlock, *J. Am. Chem. Soc.*, 1978, **100**, 4921-4922.
10. (a) M. Skibinski, R. Gomez, E. Lork and V. A. Azov, *Tetrahedron*, 2009, **65**, 10348-10354; (b) A. Iordache, M. Retegan, F. Thomas, G. Royal, E. Saint-Aman and C. Bucher, *Chem. Eur. J.*, 2012, **18**, 7648-7653.

11. (a) S. Shinkai, T. Nakaji, T. Ogawa, K. Shigematsu and O. Manabe, *J. Am. Chem. Soc.*, 1981, **103**, 111-115; (b) T. Muraoka, K. Kinbara, Y. Kobayashi and T. Aida, *J. Am. Chem. Soc.*, 2003, **125**, 5612-5613; (c) J. Wang, L. Hou, W. R. Browne and B. L. Feringa, *J. Am. Chem. Soc.*, 2011, **133**, 8162-8164.
12. (a) M. Barboiu, L. Prodi, M. Montalti, N. Zaccheroni, N. Kyritsakas and J.-M. Lehn, *Chem. Eur. J.*, 2004, **10**, 2953-2959; (b) A. Petitjean, R. Khoury, N. Kyritsakas and J.-M. Lehn, *J. Am. Chem. Soc.*, 2004, **126**, 6637-6647; (c) M. Linke-Schaetzl, C. E. Anson, A. K. Powell, G. Buth, E. Palomares, J. D. Durrant, T. S. Balaban and J. M. Lehn, *Chem. Eur. J.*, 2006, **12**, 1931-1940; (d) M. Barboiu, Y.-M. Legrand, L. Prodi, M. Montalti, N. Zaccheroni, G. Vaughan, A. van der Lee, E. Petit and J.-M. Lehn, *Eur. J. Inorg. Chem.*, 2009, **2009**, 2621-2628; (e) S. Ulrich and J.-M. Lehn, *Chem. Eur. J.*, 2009, **15**, 5640-5645; (f) S. Ulrich, A. Petitjean and J.-M. Lehn, *Eur. J. Inorg. Chem.*, 2010, **2010**, 1913-1928; (g) J. Leblond, H. Gao, A. Petitjean and J.-C. Leroux, *J. Am. Chem. Soc.*, 2010, **132**, 8544-8545; (h) X. Su, S. Voskian, R. P. Hughes and I. Arahamian, *Angew. Chem. Int. Ed.*, 2013, **52**, 10734-10739; (i) Y. Tsuchido, Y. Suzuki, T. Ide and K. Osakada, *Chem. Eur. J.*, 2014, **20**, 4762-4771.
13. B. Doistau, A. Tron, S. A. Denisov, G. Jonusauskas, N. D. McClenaghan, G. Gontard, V. Marvaud, B. Hasenknopf and G. Vives, *Chem. Eur. J.*, 2014, **20**, 15799-15807.
14. (a) T. Nabeshima, Y. Hasegawa, R. Trokowski and M. Yamamura, *Tetrahedron Lett.*, 2012, **53**, 6182-6185; (b) Y. Tanaka, K. M.-C. Wong and V. W.-W. Yam, *Chem. Eur. J.*, 2013, **19**, 390-399; (c) Y. Tanaka, K. Man-Chung Wong and V. Wing-Wah Yam, *Chem. Sci.*, 2012, **3**, 1185-1191; (d) Y. Tanaka, K. M. Wong and V. W. Yam, *Angew. Chem. Int. Ed.*, 2013, **52**, 14117-14120.
15. (a) Z. Guo, W. L. Tong and M. C. W. Chan, *Chem. Commun.*, 2009, 6189-6191; (b) Z. Guo, S.-M. Yiu and M. C. W. Chan, *Chem. Eur. J.*, 2013, **19**, 8937-8947; (c) W.-L. Tong, S.-M. Yiu and M. C. W. Chan, *Inorg. Chem.*, 2013, **52**, 7114-7124.
16. B. Doistau, A. Tron, S. A. Denisov, G. Jonusauskas, N. D. McClenaghan, G. Gontard, V. Marvaud, B. Hasenknopf and G. Vives, *Chem. Eur. J.*, 2014, DOI: 10.1002/chem.201404064.
17. R. Dobrawa, M. Lysetska, P. Ballester, M. Grunea and F. Wurthner, *Macromolecules*, 2005, **38**, 1315-1325.
18. C. M. Che, C. C. Kwok, S. W. Lai, A. F. Rausch, W. J. Finkenzeller, N. Zhu and H. Yersin, *Chem. Eur. J.*, 2010, **16**, 233-247.
19. (a) J. J. Novoa, G. Aullon, P. Alemany and S. Alvarez, *J. Am. Chem. Soc.*, 1995, **117**, 7169-7171; (b) A. Poater, S. Moradell, E. Pinilla, J. Poater, M. Sola, M. A. Martinez and A. Llobet, *Dalton Trans.*, 2006, 1188-1196; (c) A. Poater, S. Moradell, E. Pinilla, J. Poater, M. Sola, M. A. Martinez and A. Llobet, *Dalton Trans.*, 2006, 1188-1196; (d) W. B. Connick, L. M. Henling, R. E. Marsh and H. B. Gray, *Inorg. Chem.*, 1996, **35**, 6261-6265.
20. G. Anderegg and V. Gramlich, *Helv. Chim. Acta*, 1994, **77**, 685-690.
21. C. V. Banks and R. I. Bystrhoff, *J. Am. Chem. Soc.*, 1959, **81**, 6153-6158.
22. (a) K. A. Connors, in *Comprehensive Supramolecular Chemistry*, eds. J. L. Atwood, J. E. D. Davies, D. D. MacNicol and F. Vögtle, Pergamon, Oxford, 1996, vol. 3, ch. 6, pp. 205-224; (b) H.-J. Schneider and A. Yatsimirsky, *Principles and Methods in Supramolecular Chemistry*, John Wiley & Sons, Chichester, 2000; (c) P. Thordarson, *Chem. Soc. Rev.*, 2011, **40**, 1305-1323.
23. (a) S. Biswas, R. Saha and A. Ghosh, *Organometallics*, 2012, **31**, 3844-3850; (b) L. K. Das, R. M. Kadam, A. Bauza, A. Frontera and A. Ghosh, *Inorg. Chem.*, 2012, **51**, 12407-12418.
24. (a) C.-M. Che, S.-C. Chan, H.-F. Xiang, M. Chan, Y. Liu and Y. Wang, *Chem. Commun.*, 2004, 1484-1485; (b) C.-M. Che, C.-C. Kwok, S.-W. Lai, A. F. Rausch, W. J. Finkenzeller, N. Zhu and H. Yersin, *Chem. Eur. J.*, 2010, **16**, 233-247.
25. (a) S. D. Cummings and R. Eisenberg, *J. Am. Chem. Soc.*, 1996, **118**, 1949-1960; (b) W. Wu, J. Sun, S. Ji, W. Wu, J. Zhao and H. Guo, *Dalton Trans.*, 2011, **40**, 11550-11561.
26. (a) B. Ma, J. Li, P. I. Djurovich, M. Yousufuddin, R. Bau and M. E. Thompson, *J. Am. Chem. Soc.*, 2004, **127**, 28-29; (b) V. W.-W. Yam, K. M.-C. Wong and N. Zhu, *J. Am. Chem. Soc.*, 2002, **124**, 6506-6507.
27. (a) A. Lavie-Cambot, C. Lincheneau, M. Cantuel, Y. Leydet and N. D. McClenaghan, *Chem. Soc. Rev.*, 2010, **39**, 506-515; (b) X.-y. Wang, A. Del Guerso and R. H. Schmehl, *J. Photochem. Photobiol., C*, 2004, **5**, 55-77.
28. L. Farrugia, *J. Appl. Crystallogr.*, 1999, **32**, 837-838.
29. G. Sheldrick, *Acta Crystallogr., Sect. A*, 2008, **64**, 112-122.
30. M. J. Frisch, G. W. Trucks, H. B. Schlegel, G. E. Scuseria, M. A. Robb, J. R. Cheeseman, G. Scalmani, V. Barone, B. Mennucci, G. A. Petersson, H. Nakatsuji, M. Caricato, X. Li, H. P. Hratchian, A. F. Izmaylov, J. Bloino, G. Zheng, J. L. Sonnenberg, M. Hada, M. Ehara, K. Toyota, R. Fukuda, J. Hasegawa, M. Ishida, T. Nakajima, Y. Honda, O. Kitao, H. Nakai, T. Vreven, J. A. Montgomery Jr., J. E. Peralta, F. Ogliaro, M. J. Bearpark, J. Heyd, E. N. Brothers, K. N. Kudin, V. N. Staroverov, R. Kobayashi, J. Normand, K. Raghavachari, A. P. Rendell, J. C. Burant, S. S. Iyengar, J. Tomasi, M. Cossi, N. Rega, N. J. Millam, M. Klene, J. E. Knox, J. B. Cross, V. Bakken, C. Adamo, J. Jaramillo, R. Gomperts, R. E. Stratmann, O. Yazyev, A. J. Austin, R. Cammi, C. Pomelli, J. W. Ochterski, R. L. Martin, K. Morokuma, V. G. Zakrzewski, G. A. Voth, P. Salvador, J. J. Dannenberg, S. Dapprich, A. D. Daniels, Ö. Farkas, J. B. Foresman, J. V. Ortiz, J. Cioslowski and D. J. Fox, Gaussian, Inc., Wallingford, CT, USA, 2009.



80x39mm (300 x 300 DPI)